

THE OROGENIC GOLD POTENTIAL OF THE CENTRAL LAPLAND GREENSTONE BELT, NORTHERN FENNOSCANDIAN SHIELD

10.2

T. Niiranen, I. Lahti, V. Nykänen

ABSTRACT

The Paleoproterozoic Central Lapland Greenstone Belt (CLGB) hosts a number of orogenic gold deposits, the total reported gold endowment being 9.1 Moz. Genetic models of the orogenic gold deposits suggest that the gold source for these deposits is the rocks undergoing metamorphism at depth. If a metamorphic source model is applied to the Kittilä terrane, comprising the core of the Central Lapland Greenstone Belt, potentially as much as 30 times the currently known gold resource was mobilized from the up to 9-km-thick metavolcanic rock sequence comprising the terrane. The size distribution of orogenic gold deposits in gold districts with long exploration histories follows a consistent nonlinear pattern. In comparison, the size distribution of the Central Lapland Greenstone Belt is highly skewed, indicating that the number of gold deposits, including deposits in the 0.5–1.5 Moz size category, remain undiscovered in the belt. The study shows that the Central Lapland Greenstone Belt is underexplored and that the remaining orogenic gold potential of the belt is significant.

Keywords: Orogenic gold deposits; greenstone belts; Paleoproterozoic; 3D modeling; Fennoscandian Shield; Finland.

INTRODUCTION

Orogenic gold deposits are typically the dominant gold source in metamorphosed greenstone and sedimentary belts. More than 100 Moz of gold have been produced from some of the most renowned gold provinces, including the Superior Province in Canada, the West African craton, the Yilgarn craton in east Australia, and the Lachlan Fold belt in western Australia (e.g., Goldfarb et al., 2001). At camp and district scale, known deposits cluster in proximity to transcrustal or other major deformation zones that are formed synchronously with the thickening of the crust during accretionary or collisional tectonic events. In most prospective districts, the deposits were formed at mid-crustal levels as suggested by the dominant greenschist facies metamorphic assemblages of the host rocks.

Genetic models for orogenic gold deposits have been discussed in several studies (e.g., Groves et al., 1998; McCuaig and Kerrich, 1998; Goldfarb et al., 2001; Groves et al., 2003; Philips and Powell, 2010). The key aspects of these models are: (1) metals, complexing agent(s), and fluids transporting the

metals are released from the source (or sources) at depth, (2) metal carrying fluids are focused into shear zones, and (3) the auriferous fluids migrate along structures into suitable structural and/or chemical traps where the gold and associated metals are deposited via various physicochemical reactions. The ultimate sources of these fluids, metals, and complexing ligands have been under considerable discussion, with models ranging from entirely magmatic to purely metamorphic sources to somewhere in-between. The metamorphic source models suggest that the gold and gold-carrying fluids are released from rocks undergoing prograde metamorphism related to accretionary orogenic events (e.g., Goldfarb et al., 2005).

Studies by Pitcairn et al. (2006) and Pitcairn (2012) show that the background concentrations of gold drop systematically with increasing metamorphic grade. It has also been shown that metamorphic devolatilization reactions in mafic rock sequences at the greenschist–amphibolite facies transition produce significant quantities of low salinity, near-neutral H_2O – CO_2 – H_2S fluids characteristic of orogenic gold deposits (Philips and Powell, 2010). Thus, it is possible that all metals, complexing ligands, and fluids related to orogenic gold deposits are products of devolatilization reactions of the rocks undergoing metamorphism at depth and that magmatic sources are not involved. The role of subducting crust and enriched subcontinental lithospheric mantle as the bulk source for gold and gold-carrying fluids has been emphasized by some authors (e.g., Groves et al., 1998; Goldfarb et al., 2005) and the evidence from certain gold districts (e.g., Jiandong, China) suggests that the subducting crust appears to be the most likely source in some districts (Goldfarb and Santosh, 2014).

The orogenic gold deposits of the world include some giant (>250 t Au) and numerous world class (>100 t Au) deposits. In well-explored gold districts, the known deposits appear to follow a size distribution pattern where the total gold endowment of a district is divided among one to a few large deposits, a group of mid-sized deposits, and a large number of smaller deposits. For example, the Abitibi belt hosts three giant deposits, one world-class deposit, a total of seven 1–3 Moz deposits, and 25 deposits with <1 Moz Au (Gosselin and Dubé, 2005). Similar distribution patterns can be found in other well-explored gold districts; for example, greenstone belts in Yilgarn and Zimbabwe cratons (Gosselin and Dubé, 2005).

A number of orogenic gold deposits are known in Archean and Paleoproterozoic greenstone and schist belts of the Fennoscandian Shield (e.g., Eilu et al., 2003). One of the most prospective belts for orogenic gold, indicated by currently known total gold resources in excess of 9 Moz, is the Central Lapland Greenstone Belt (CLGB), which is the most extensive Paleoproterozoic volcano-sedimentary belt in Europe. It extends approximately 450 km from northern Norway through Finland into Russian Karelia to the south (Fig. 10.2.1). Active gold exploration in the CLGB started in the early 1980s and since then several gold deposits have been discovered within the belt (Eilu et al., 2007). The known gold deposits (e.g., Eilu et al., 2012) are most numerous within and at the southern contact of the Kittilä terrane, forming the central core of the CLGB, but gold occurrences are known throughout the belt.

Currently, the most significant gold deposit in the CLGB is the world-class Suurikuusikko deposit, with total resources at the end of 2013 of 7.67 Moz (Agnico Eagle Ltd., 2013). The Suurikuusikko deposit alone represents 84% of the total reported gold endowment of the CLGB, while the second largest deposit, Pahtavaara, has only 0.37 Moz gold (Table 10.2.1). This highly skewed size distribution most likely reflects the relatively short exploration history of the CLGB and suggests that the amount of undiscovered gold in the CLGB may be considerable.

Various methods have been used to estimate undiscovered metal resources in certain districts. These include the three-part quantitative mineral-resource assessment method (Singer, 1993; Singer and Manzie, 2010). Such estimation was carried out for orogenic gold deposits in northern Finland, suggesting that

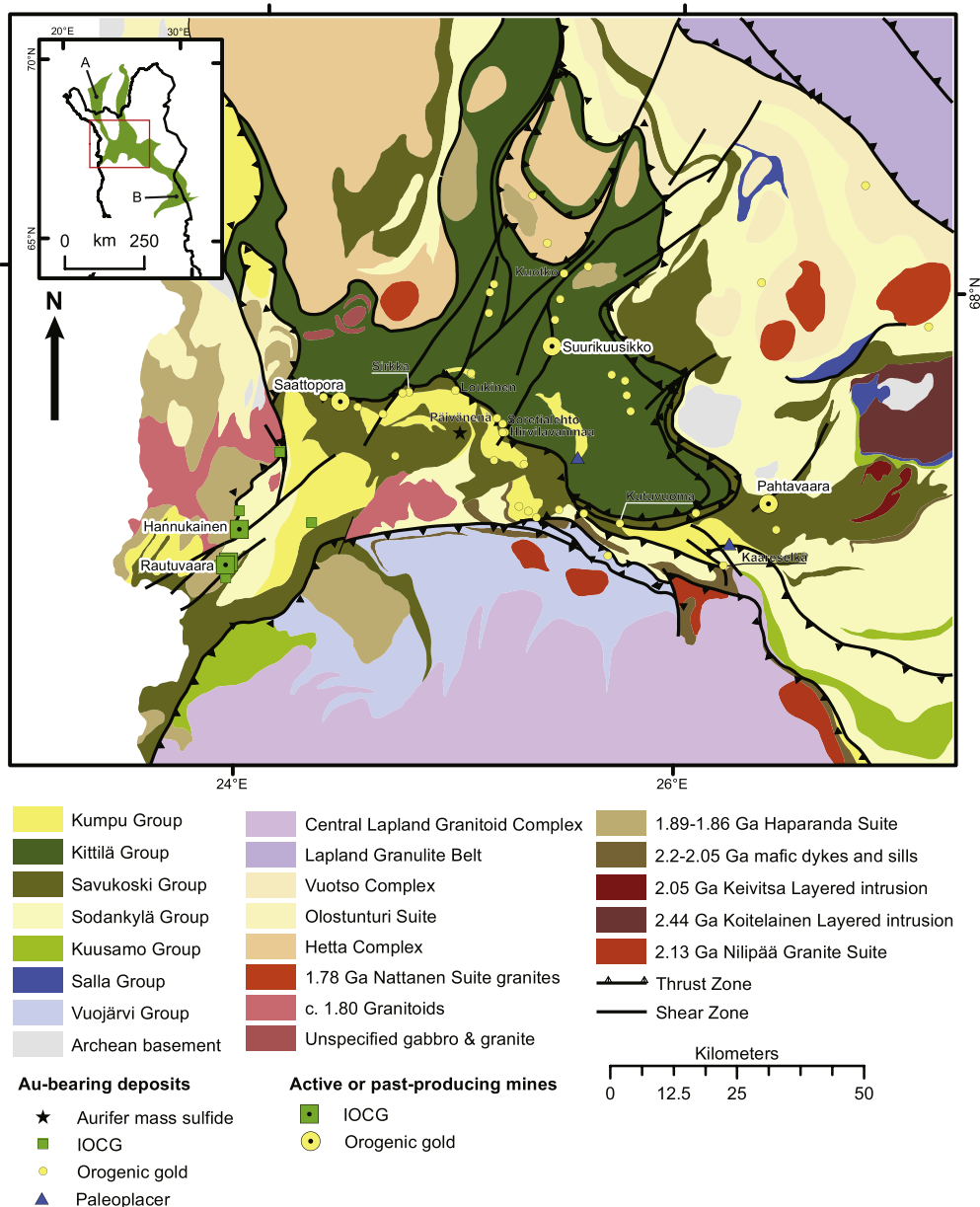


FIGURE 10.2.1 Location of the study area with extent of the Central Lapland Greenstone Belt (green) and location of (A) Bidjovagge and (B) Juomasuo deposits (inset).

Main geological units and location of the known gold deposits.

Source: Modified from GTK *Bedrock of Finland – DigiKP* (October 15, 2013) and *FINGOLD* (October 15, 2013).

Table 10.2.1 Orogenic gold deposits with reported resources within the CLGB

Deposit	Mineralization style	Host rock(s)	Metal association	Size (Mt)	Au (g/t)	Resources (oz)	References
Suurikuusikko	Refractory Au in disseminated arsenopyrite and pyrite	Albitized KiG metatholeiite and argillite	Au-As Ag, Bi, Co, Sb, Se, W	56.07	4.25	7,665,129	a, b
Pahtavaara ¹	Qtz-barite-Au lenses and pods	Altered metakomatiite of SaG	Au-Ba, Ag, B, Te, W	4.98	2.29	367,742	a, d
Bidjovagge	Native gold with sulfides in qtz-carb-veins and breccia	Albitized dolerite and graphitic phyllite (corresponding SaG)	Au-Cu, Te, U	3.31	2.87	306,452	d
Juomasuo ¹	Native gold associated with disseminated sulfides and uraninite	Multiply altered SoG quartzite and meta-arkose	Au-Co-Cu-U-LREE, As, Ba, Bi, Mo, Ni, Se, Te, Th, U, W, Y	1.96	4.90	305,600	a, c
Saattopora	Native gold with sulfides in qtz-carb-veins and breccia	Albitized SaG phyllite	Au-Cu, Ag, As, B, Bi, Se, Te, U, W	2.16	2.91	203,226	a, d
Kuotko	Native and refractory gold with sulfides in qtz-carb-veins and breccia	Albitized KiG metatholeiite and argillite	Au-As-Bi, Te, W	1.82	2.89	170,044	a, b, d
Kaaretselkä	Native gold with sulfides in qtz-carb-veins and disseminated sulfides in altered wall rocks	Albitized SaG metatuffites and phyllites	Au-Cu, As	0.30	5.00	48,387	a, d
Kettukuusikko	Native gold with sulfides in qtz-carb-veins	Altered SaG metakomatiite	Au-Cu, Ag, Ni, Sb, Se	0.44	1.80	25,548	a, d
Kutuvuoma	Native gold with sulfides in qtz-carb-veins	Altered SaG metakomatiite and graphitic phyllite	Au-Cu, As, Co, Ni	0.07	6.70	14,697	a, d
Hirvilavanmaa	Native gold with sulfides in qtz-carb-veins and breccia	Altered SaG metakomatiite	Au, Ni, Sb, Te	0.11	2.90	10,290	a, d
Sirkka	Native gold with sulfides in qtz-carb-veins and breccia	Albitized SaG phyllite, mafic metalava, and metakomatiite	Au-Co-Cu-Ni, As	0.25	0.80	6452	a, d
Loukinen	Native gold with sulfides in qtz-carb-veins and breccia	Albitized SaG graphitic-phyllite	Au-Ni, Ag, As, Co, Cu	0.11	0.50	1839	a, d
Soretialehto	Native gold with sulfides in qtz-carb-veins and breccia	Altered SaG metakomatiite	Au, As, W	0.01	3.50	1468	a, d

Resources reported with total in situ including reserves, resources, and mined resources (where applicable). KiG = Kittilä group, SaG = Savukoski group, SoG = Sodankylä group

¹Other genetic type(s) proposed.

^aEilu et al. (2007)

^bwww.agnico-eagle.com

^cwww.dragon-mining.com.au

^dEilu et al. (2012)

with 50% certainty, the total gold endowment in northern Finland as a whole is at least 290 tonnes or 9.4 Moz (Rasilainen et al., 2012). In the same study, the estimated undiscovered gold resources of the Kittilä terrane are 45 tonnes (1.4 Moz). A spatial mineral prospectivity assessment using methodologies described by Bonham-Carter (1988) was performed by Nykänen et al. (2008). This study delineated several high prospectivity areas for orogenic gold deposits within the current study area; however, it does not contain a quantitative estimate for the undiscovered gold resources.

In the work reported here, the gold potential of the Kittilä terrane and CLGB is estimated using two different approaches. The first approach applies a metamorphic source model for the orogenic gold deposits that assumes that all the metals and fluids related to the deposits in CLGB are released from the rocks undergoing metamorphism at depth. This model is applied to the Kittilä terrane for which a geologic 3D model is constructed based on the available seismic and gravity data. The total amount of gold mobilized from the Kittilä terrane rocks is estimated based on the data by Pitcairn et al. (2006) and Pitcairn (2012) for gold depletion in sedimentary and volcanic rocks during prograde metamorphism, and the volumes of Kittilä terrane rocks based on the geological 3D model created in this work.

In a second approach, the gold potential of the CLGB is estimated by a statistical comparison with some of the best-known orogenic gold-hosting greenstone belts with prolonged exploration history around the world. The size distributions of the orogenic gold deposits in the Abitibi (Canada), Norseman-Wiluna (Australia), and Zimbabwe greenstone belts are studied for any consistencies between these belts, and a comparison is made with the CLGB. The data for deposit size by Gosselin and Dubé (2005) is used for these belts. Although it is approximately 10 years old and, thus, somewhat outdated, it is probably the most coherent dataset available and still suitable for the purposes used in this work.

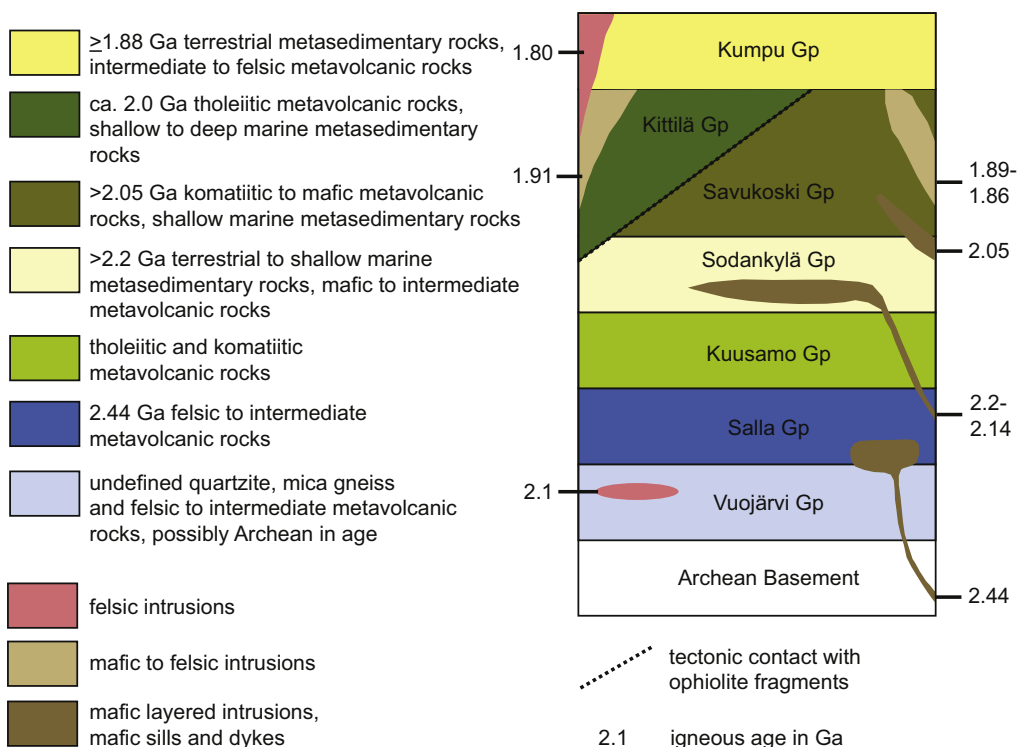
GENERAL GEOLOGICAL FEATURES OF THE CENTRAL LAPLAND GREENSTONE BELT

The geology of the central part of the CLGB and its immediate surroundings is shown in Fig. 10.2.1. The current geological features of the CLGB result from a multistage rifting history between 2.44 and 2.0 Ga followed by multiphase compressional and metamorphic events related to the Svecofennian orogeny at 1.91–1.79 Ga. The supracrustal units of the CLGB can be divided into two main units; the Karelian 2.44–2.0 Ga rift-related metamorphosed volcano-sedimentary sequence deposited on the Archean basement and the 1.89–1.77 Ga Svecofennian sequence dominated by clastic metasedimentary units (Lehtonen et al., 1998; Hanski et al., 2001; Hanski and Huhma, 2005). The Karelian and Svecofennian units are bounded by the migmatites and granites of Central Lapland Granitoid Complex in the south; gneisses of the Olostunturi suite, intrusions of the Haparanda suite, and ~1.80 Ga granitoids in the west; reworked Archean gneisses of the Hetta complex in the north; and high-metamorphic-grade rocks of the Lapland granulite belt and Vuotso complex in the northeast (Lehtonen et al., 1998; Hanski and Huhma, 2005; Fig. 10.2.1).

STRATIGRAPHY

The supracrustal rocks of the CLGB are divided into seven lithostratigraphical units or groups: the Vuojärvi, Salla, Kuusamo, Sodankylä, Savukoski, and Kittilä groups comprising the Karelian units and the Kumpu group in the Svecofennian unit (Fig. 10.2.2). The Salla group is the oldest unit exposed in the eastern and

Central Lapland Greenstone Belt

**FIGURE 10.2.2 Stratigraphy and main igneous events of the Central Lapland Greenstone Belt.**

Archean basement consists of tonalite-trondhjemite-granodiorite (TTG) series rocks.

Source: Compiled after *Hanski et al. (2001)* and *Bedrock of Finland – DigiKP (October 15, 2013)*.

southeastern part of the CLGB and consists of 2.44 Ga felsic metavolcanic rocks deposited on the metamorphosed Archean basement (*Lehtonen et al., 1998*). The Vuojärvi group rocks, located at the southern margin of the CLGB, consist of quartz-feldspar-sericite schists and gneisses of uncertain origin. The felsic metavolcanic rocks of the Salla group, together with the 2.44 Ga layered intrusions, resulted from the initial rifting phase of the Archean in the area (*Hanski and Huhma, 2005; Lahtinen et al., 2005*).

The Salla and Vuojärvi groups are overlain by extensive mafic metavolcanic rocks of the 2.2–2.44 Ga Kuusamo group. This volcanic activity was followed by a more tranquil phase resulting in deposition of thick and extensive epiclastic sequences of the Sodankylä group, dominated by quartzites and meta-arkoses with only minor mafic metavolcanic rock intercalations. The 2.05–2.2 Ga Savukoski group overlying the earlier units consists of fine-grained metasedimentary rocks including phyllites, mica schists, graphite- and sulfide-bearing schists, and metatuffites, and tholeiitic metavolcanic rock intercalations suggest deepening of the depositional basin. The komatiitic to picritic metavolcanic rocks, which represent the uppermost part of the Savukoski group, and abundant 2.2 and 2.05 Ga mafic dikes and sills suggest further rifting of the basin. The Kittilä group comprises the youngest Karelian

unit of the CLGB. It consists of a thick sequence of tholeiitic metavolcanic rocks with passive margin and oceanic affinity and minor metasedimentary intercalations of argillites, graphite- and sulfide-bearing schists, and banded iron formations (Lehtonen et al., 1998; Hanski and Huhma, 2005).

The age data of the Kittilä group metavolcanic rocks and felsic porphyry dikes crosscutting them indicate that the Kittilä group rocks were deposited at 2.015 ± 0.002 Ga (Hanski and Huhma, 2005). The Kittilä group is bound against the surrounding sequences by tectonic contacts (see Fig. 10.2.1). Hanski (1997) interpreted the Nuttio serpentinite pods located near the eastern margin of the Kittilä group as ophiolite fragments and suggested that the Kittilä group rocks represent an allochthonous unit that is at least partly oceanic in origin. Based on this and the distinct geochemical and isotopic features of the Kittilä group (e.g., Hanski and Huhma, 2005), it is referred to here as the Kittilä terrane. The youngest stratigraphical unit of the CLGB, the Kumpu group, consists of quartzites, conglomerates, and minor felsic metavolcanic rocks that overlie the Karelian rocks (Fig. 10.2.1; Lehtonen et al., 1998). U-Pb zircon data of the felsic metavolcanic rocks give an age of 1880 ± 8 Ma, being consistent with the ~ 1880 Ma detrital zircon populations obtained from the metasedimentary rocks and the 1888 ± 22 Ma age of a granitoid pebble in conglomerate from the Kumpu group (Hanski et al., 2001; Rastas et al., 2001).

INTRUSIVE MAGMATISM

The early intrusive magmatism in the area consists of 2.44 Ga and 2.05 Ga mafic layered intrusions and mafic dikes at 2.2 Ga, 2.05 Ga, and 2.0 Ga (Lehtonen et al., 1998; Hanski et al., 2001). The 2.2 Ga mafic dikes and sills occur as an east–west trending zone chiefly in the Sodankylä group rocks in the southern part of the CLGB (Fig. 10.2.1). The 2.05 Ga and 2.0 Ga magmatism consist of mafic dikes and small gabbroic intrusions, although in places coeval felsic quartz-feldspar porphyry dikes have been detected (e.g., Lehtonen et al., 1998; Hanski and Huhma, 2005). The most voluminous intrusive rocks in the area relate to the 1.91–1.86 Ga Haparanda suite felsic and mafic magmatism and 1.82–1.79 Ga granitoids. The Nilipää suite granites, which occur along the southern margin of the CLGB, have an enigmatic age of 2.1 Ga, suggesting that they were intruded during or between the extensional stages (Hanski et al., 2001).

DEFORMATION AND METAMORPHISM

The CLGB records a complex multistage deformation history which, despite numerous studies, is still not completely understood. The following sequence of deformation events is modified after the interpretations of Ward et al. (1989), Lehtonen et al. (1998), Väisänen (2002), Tuisku et al. (2006), Hölttä et al. (2007), and Patison (2007). The deformation history of the CLGB area is divided into three ductile stages followed by a completely brittle stage. The main deformation stages D1 and D2 lack clear overprinting relationships and absolute age constraints and therefore are grouped here as D1–2 stage. The D1–2 stage relates to thrust tectonics that formed the main ductile deformation features of the CLGB. The D1–2-stage features indicate south–southwest vergent transport and north–northeast vergent transport in the northern and southern part of the CLGB, respectively. The south–southwest vergent thrusting in the north relates to the collision of the Karelian and Kola cratons and thrusting of the Lapland granulite belt to the southwest. The northward-directed thrusting involved initial generation of south-dipping thrust zones at the southern margin of the area (Fig. 10.2.1). It is currently unknown if the two thrusting events were contemporaneous or successive events.

The D3-stage deformation features have highly variable vergence depending on the location, and possibly D3 consisted of several stages that were not necessarily related to each other. The D3-stage deformation features include north- to northeast-striking shear zones and local refolding of the earlier deformation features. Robust timing of the D3 stage is lacking, but a minimum age can be set as the maximum age for the subsequent brittle D4 stage at 1.77 Ga (Väisänen, 2002). The best estimates for D3 ages are 1.89–1.86 Ga or 1.82–1.77 Ga, but this may vary in different parts of the CLGB (e.g., Väisänen, 2002; Patison, 2007).

The peak metamorphic conditions in the CLGB were reached during the D1–2 stage, and represent mid-greenschist facies excluding the northernmost parts and western margin (Hölttä et al., 2007). Metamorphic grade increases south from the Kittilä terrane reaching upper amphibolite facies close to the Central Lapland Granitoid Complex rocks, and westward reaching mid-amphibolite facies at the western margin. The peak metamorphic temperature estimates for the Kittilä terrane are approximately 350 °C, although no reliable pressure estimates exist for the lowest grade metamorphic areas (Hölttä et al., 2007). The western margin of the Kittilä terrane was metamorphosed to higher temperature due to heat flow from adjacent granitoids. Thermobarometry data from this area yield a pressure-temperature (P-T) estimate of 3.2 kbar and 550 °C (Hölttä et al., 2007).

GOLD DEPOSITS

A number of gold deposits and occurrences are known within the study area (refer to Fig. 10.2.1). The deposits fall into four different genetic types, of which the orogenic type is by far the most numerous. A total of 43 orogenic gold deposits are known within the study area, although only 4 of them—Saattopora, Pahtavaara, Suurikuusikko, and Kuotko—have been mined or are planned to be mined in the near future. The remaining deposits are currently uneconomic, although some of these are under active exploration by various companies operating in the area and may prove to be economic in the future.

Most of the deposits classified as orogenic gold deposits display clear features of the deposit type as outlined by Groves et al. (1998). However, Pahtavaara is somewhat enigmatic (e.g., Eilu et al., 2003; Eilu et al., 2007; Patison et al., 2007). It was initially classified as an orogenic gold deposit by Korkiakoski (1992), but recently, alternative genetic models have been proposed (Eilu et al., 2007). The general features of the CLGB orogenic gold deposits with resource estimates are shown in Table 10.2.1. Significant gold deposits in the CLGB, but located outside of the study area, include the Bidjovagge orogenic gold deposit in the northwesternmost extension of the belt in Norway, and a group of enigmatic Au-Co-Cu-U-REE deposits, including the Juomasuo deposit in the Kuusamo district, part of the southeastern CLGB. For the Kuusamo deposits, several genetic models, including orogenic gold, have been proposed (e.g., Vanhanen, 2001; Eilu et al., 2003; Eilu et al., 2007).

DATA AND METHODS

The regional gravity survey data of the Geological Survey of Finland (GTK) was used in this work. The average observation density of the dataset is about 1–6 sites/km². Data acquisition has been made primarily using the Scintrex CG-3 and CG-5 Worden gravity meters. The Kittilä area observations started in 1972 and the latest measurements used in this work were taken in the summer of 2009. The total number of gravity observations used is 19,273. The density of gravity observations is primarily 1–4 sites per km² with the highest density being in the northern and northwestern parts of the study area.

Two sets of seismic data were used in this work (Fig. 10.2.3). The Finnish Reflection Seismic Experiment 2001–2005 (FIRE) data consist of two profiles covering 220 line-km in the study area and the High Resolution Reflection Seismics for Ore Exploration 2007–2010 (HIRE) data consist of seven profiles totaling 116 line-km. The data acquisition and processing of each dataset is described in Kukkonen et al. (2006) and Kukkonen et al. (2011). The initial 2D interpretation of the FIRE profiles was presented by Patison et al. (2006).

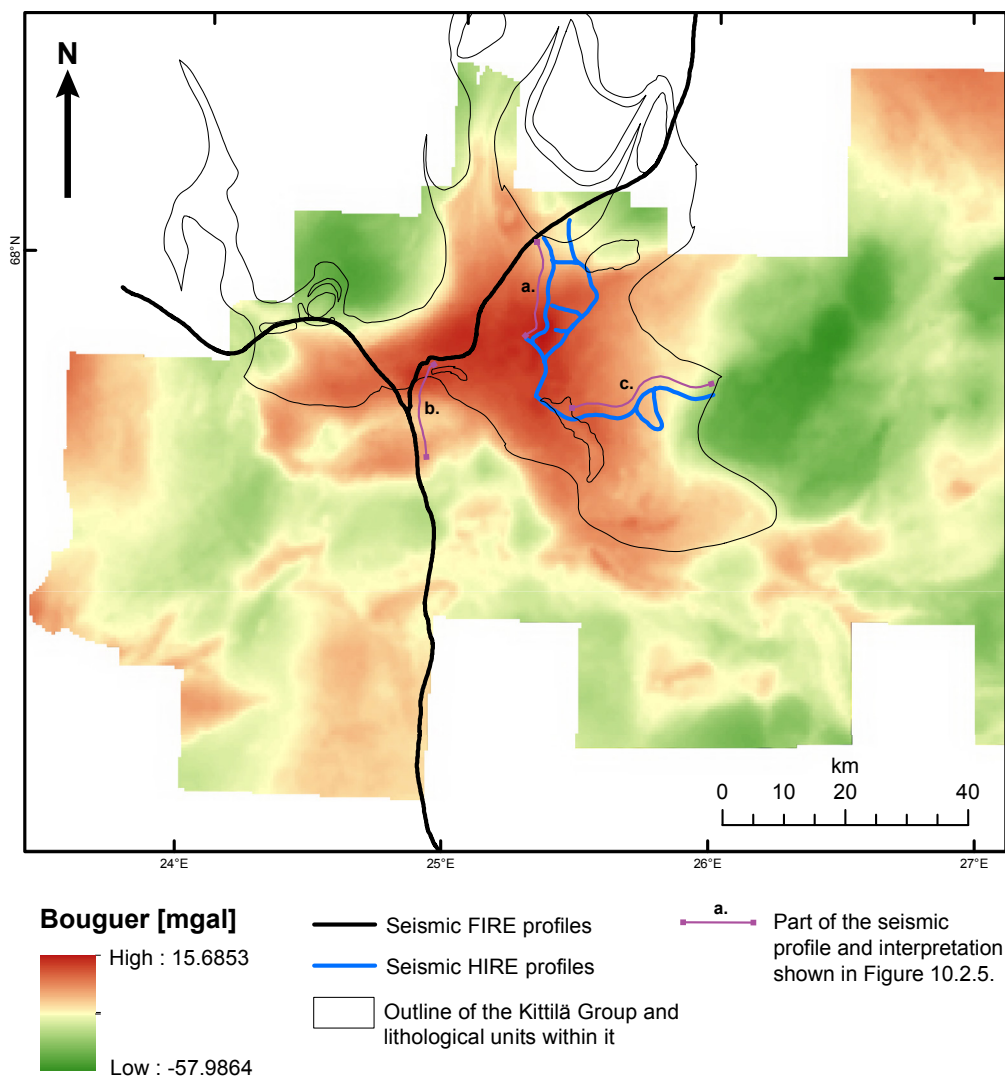


FIGURE 10.2.3 Bouguer map of the area with location of seismic profiles used in this work and outline of the Kittilä terrane.

Location of the seismic sections presented in Fig. 10.2.5.

The surface contacts of the Kittilä terrane were outlined from geological and aerogeophysical maps, and the base of the terrane from seismic profiles and using the 3D-forward model constructed using the gravity data. The final 3D model of the base of the Kittilä terrane was interpolated using the discrete smooth interpolation (DSI) method built into GOCAD® software.

3D MODEL OF THE KITILÄ TERRANE

Three-dimensional gravity modeling was carried out to obtain information on the deep geometry of the Kittilä terrane and adjacent areas (Fig. 10.2.4). The terrane is favorable for gravity modeling as it produces a significant positive Bouguer anomaly of ~45 mGal. The anomaly is caused by thickness variations of the higher-density mafic metavolcanic rocks of the terrane in contrast to the lower-density background rocks such as granitoids, quartzites, and schists.

The regional Bouguer gravity data were gridded and modeling profiles were created by sampling the grid along 20 north–south oriented, 80-km-long lines, spaced 5 km apart. The model area is 95 km east–west by 80 km north–south. The model was constructed from a number of layer-type, three-dimensional bodies as shown in Fig. 10.2.4. Due to thousands of bedrock and drill hole observations, the surface geology of the target area is relatively well known. Therefore, the topmost part of the model is primarily based

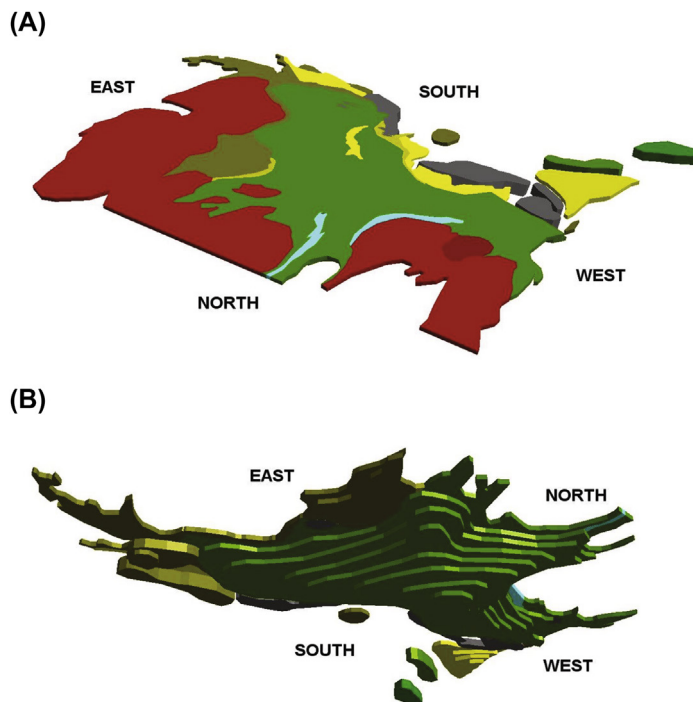


FIGURE 10.2.4 Three-dimensional gravity model of the terrane area.

Perspective view from (A) northwest and (B) northeast. Model colors denote various densities used in the modeling.

on lithological maps. Model densities, geometries, and regional trends were modified manually to improve the fit between the measured and calculated data along the modeled profiles. Although such a “trial and error” forward modeling procedure is time consuming, it allows control so that the results can be modified to best fit geological and geophysical constraints during the modeling process.

The model was revised several times in 3D together with reflection seismics to get good agreement between the dip angles and directions of dipping reflectors. In seismic profiles, the boundary between the Kittilä terrane and adjacent units shows up as an unconformable zone between the subhorizontal reflectors, and in some places as transparent nonreflective zones representing shear or thrust zones truncating the reflectors (Fig. 10.2.5). In places, the contact is located in zones with conformable reflectors or it is difficult to outline in the seismic data without the use of the gravity model (Fig. 10.2.5).

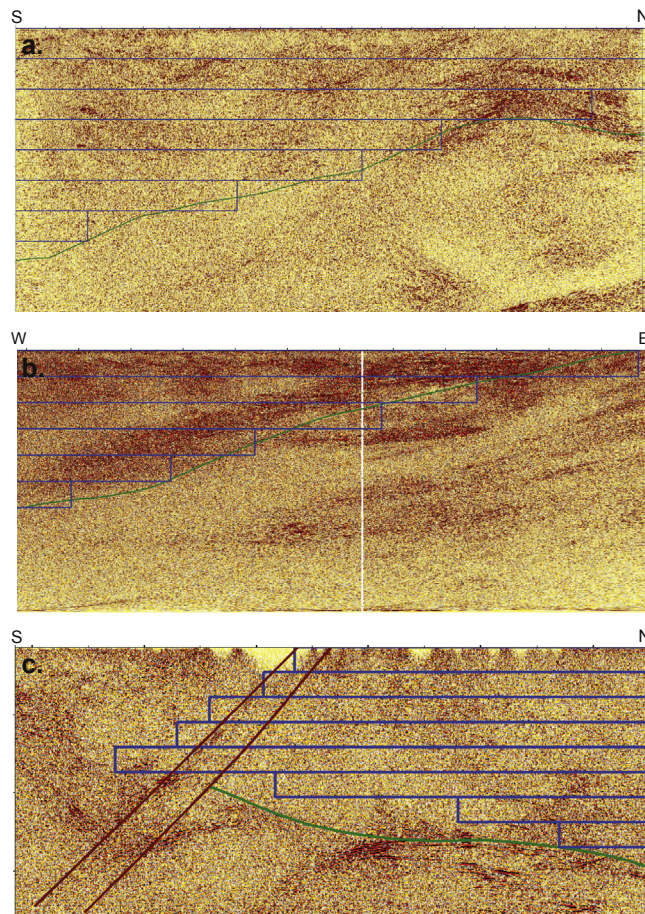


FIGURE 10.2.5 Examples of the seismic interpretation of the base of the Kittilä terrane.

The base is drawn in green, blue lines represent the 3D forward model layers, and brown lines in panel c. represent the Sirkka thrust zone structures outlining the southern margin of the unit. Locations of the sections a., b., c. shown in Fig. 10.2.3. Vertical extent of the seismic profiles is 10 km in all panels.

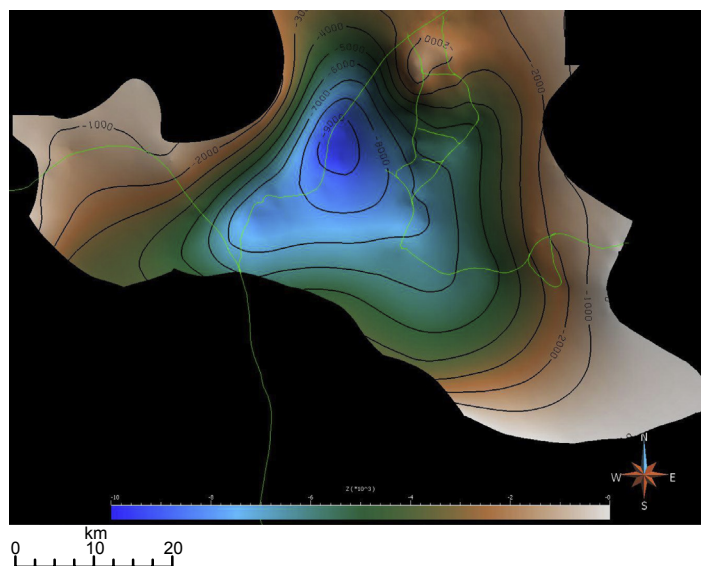


FIGURE 10.2.6 Modeled base of the Kittilä terrane with depth contours in meters below current erosional level, which is set to zero.

To get a better final modeling result, the most significant geological units around the terrane were incorporated into the 3D gravity model. The area is characterized by granitoids to the north and east, which cause negative Bouguer anomalies. Densities of $2600\text{--}2650\text{ kg/m}^3$ and thicknesses of $1\text{--}6\text{ km}$ were used for granitic intrusions to fit these negative Bouguer anomalies. To the south of the Kittilä terrane, denser rock types such as schist, mica schist, and mafic–ultramafic intrusions create short wavelength-positive anomalies. Consequently, higher density blocks ($2650\text{--}3050\text{ kg/m}^3$) were added in the southern part of the model. The Kittilä terrane was modeled using a density of 2950 kg/m^3 , representative of mafic metavolcanic rocks in the study area. A background density of 2780 kg/m^3 was assigned for the rest of the 3D model as this value represents an average between the mafic and felsic rock types encountered in the area. Several smaller-scale high- or low-density bodies were necessary to add to the terrane model. These anomalies are caused by Kittilä terrane banded iron formations, overlying Kumpu group quartzites and granitoid intrusions.

The final 3D model of the base of the Kittilä terrane is shown in Fig. 10.2.6. Based on the model, the thickness of the unit varies considerably: up to 9-km thick in the central parts but thinning dramatically to the west, north, and southeast. The terrane is up to 5-km thick at its southern margin where it is cut by the south-dipping Sirkka thrust zone.

ESTIMATION OF THE QUANTITY OF GOLD MOBILIZED FROM THE KITILÄ TERRANE ROCKS

The 3D model of the Kittilä terrane, combined with the metamorphic data, allows rough estimates to be made on the potential quantity of gold mobilized from the rocks during regional metamorphism.

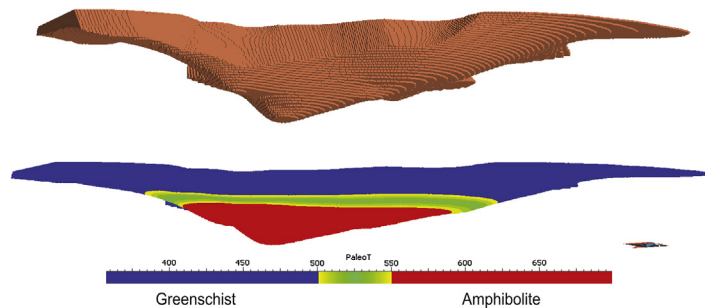


FIGURE 10.2.7 Voxet model of the Kittilä allochthon and calculated peak metamorphic conditions.

The transition zone (500–550 °C) between greenschist and amphibolite facies is shown as a green-yellow zone. Total volume of the Kittilä terrane rocks in amphibolite facies (>525 °C) is approximately 1500 km³. View to the north.

The method for this estimate follows the studies by [Pitcairn et al. \(2006\)](#) and [Pitcairn \(2012\)](#), which show that the gold concentrations of nonmineralized rocks decrease systematically with increasing metamorphic grade and that the drop is most dramatic at the boundary between greenschist and amphibolite facies. Their data indicate that rocks metamorphosed at amphibolite facies contain between 50% and 80% less gold than their nonmineralized, unmetamorphosed protoliths. Based on the peak metamorphic estimates by [Hölttä et al. \(2007\)](#), the temperature gradient during metamorphism in the Kittilä area was 37 °C/km, close to a typical Barrovian-type metamorphism. The data on the metamorphic conditions for the Kittilä terrane presented by [Hölttä et al. \(2007\)](#) indicate that the peak metamorphic conditions were approximately 350 °C in the central and southern parts of the area. Using these values, the greenschist-amphibolite facies transition zone at 500–550 °C occurs between 4.05–5.35 km depth below the current erosional level. This transition zone is modeled in the voxet model of the Kittilä terrane shown in [Fig. 10.2.7](#). The total volume of the Kittilä terrane below the greenschist-amphibolite facies zone is approximately 1500 km³, which equals 4.425×10^{12} tonnes using a density of 2950 kg/m³.

No measured data exist on the background Au concentration of the Kittilä terrane rocks. Data from the literature suggest that the mean gold concentration of the unmetamorphosed basalts (excluding continental flood basalts) varies between 0.75 and 4.7 ppb depending on the chemical affinity of the basalt ([Pitcairn, 2012](#), and references therein). As the bulk of the Kittilä terrane consists of tholeiitic metabasalts, a background Au concentration of 2 ppb was used in calculations. Using this value and the calculated tonnage of the Kittilä terrane rocks below the greenschist-amphibolite facies boundary, some 4425–7080 tonnes or 143–228 Moz of Au may have been mobilized just from the Kittilä terrane rocks using gold mobilization efficiencies of 50–80%.

COMPARISON OF THE GOLD ENDOWMENT OF THE CLGB TO WELL-EXPLORED GREENSTONE BELTS WORLDWIDE

Besides geology and size, the known gold endowment of a certain region is highly dependent on the exploration maturity of the area. Gold exploration in the CLGB has only been active for the relatively short period of about 30 years. The currently reported gold endowment related to orogenic gold

deposits is 9.1 Moz hosted by 13 deposits (Table 10.2.1). For comparison, data on orogenic gold deposits from greenstone belts in the Zimbabwe craton, Abitibi greenstone belt, and Norseman-Wiluna belt are presented in Fig. 10.2.8. All of these are well-known gold districts with 100+ years of exploration history. The extent of the greenstone belts is shown in Fig. 10.2.9. There are differences in the sizes of the belts; the Abitibi belt is the least extensive, yet the total gold endowment of it is the largest of the three. The CLGB has roughly the same extent as the Abitibi belt. The data of each district show size distributions of deposits, which appear to follow near logarithmic patterns. The districts have variably harmonic patterns: the Zimbabwe craton and Abitibi belt data are most harmonic and the Norseman-Wiluna belt is somewhat less harmonic.

The data for each belt were plotted on bivariate diagrams where the x -axis represents the deposit size in Moz and the y -axis is the ordinal number of the deposit from the largest to the smallest, normalized by the number of deposits in each dataset (Fig. 10.2.10). A regression line following the function

$$y = ax^{-b} \quad (10.2.1)$$

was fitted to each of the datasets, with a and b being constants of which b reflects the skew of the data and a the total gold endowment of the district.

The fit of the regression lines for the Zimbabwe craton and Abitibi and Norseman-Wiluna belt data is good, with correlation coefficients of 0.94 or higher. Based on the data of the selected districts, it appears that the size distribution of orogenic gold deposits in gold districts with prolonged gold exploration history follow a pattern similar to the Gutenberg–Richter law, describing the relationship between magnitude and total number of earthquakes in any given seismic region (Gutenberg and Richter, 1949). In seismology, the constant b of Equation (10.2.1) varies between 0.5 and 1.5, being typically close to 1 (i.e., close to log-normal) and the Gutenberg–Richter law based regression has been used to predict numbers and magnitudes of earthquakes in given districts.

In contrast to that just described, a similar regression line fitted to the CLGB data shows a poor fit, both constants of Eq. (10.2.1) being unreasonable (Fig. 10.2.10). Thus, it is obvious that the dataset is too small. For comparison, the shaded area covering the calculated regression lines of the other datasets is shown. Poor fit at the smaller deposit end of the CLGB data to the shaded area is due to differences in the datasets, as the CLGB data includes data from subeconomic occurrences (<0.1 Moz) that are not included in other datasets. If the subeconomic deposits are omitted from the CLGB data, the smaller deposits of the curve would fit relatively well to the regression lines defined by other areas. However, the Suurikuusikko deposit plots well outside this area. For the CLGB data to better fit the distribution of the other belts, the dataset should contain a significantly higher number of deposits including ones in the 0.5–1.5 Moz size range.

DISCUSSION

The 3D model of the Kittilä terrane presented in Fig. 10.2.7 shows that thickness of the unit varies from 0–9 km. The variation is likely a result of considerable deformation of the unit during the southwest- and north-vergent thrusting events related to the main deformation phases of the Svecofennian orogeny and subsequent erosion. The Kittilä terrane has been considered to represent, at least partially, an allochthonous unit based on geochemical characteristics. The presence of serpentinite pods near the eastern margin is interpreted to represent ophiolite fragments and the tectonic or, at least, tectonized character of unit

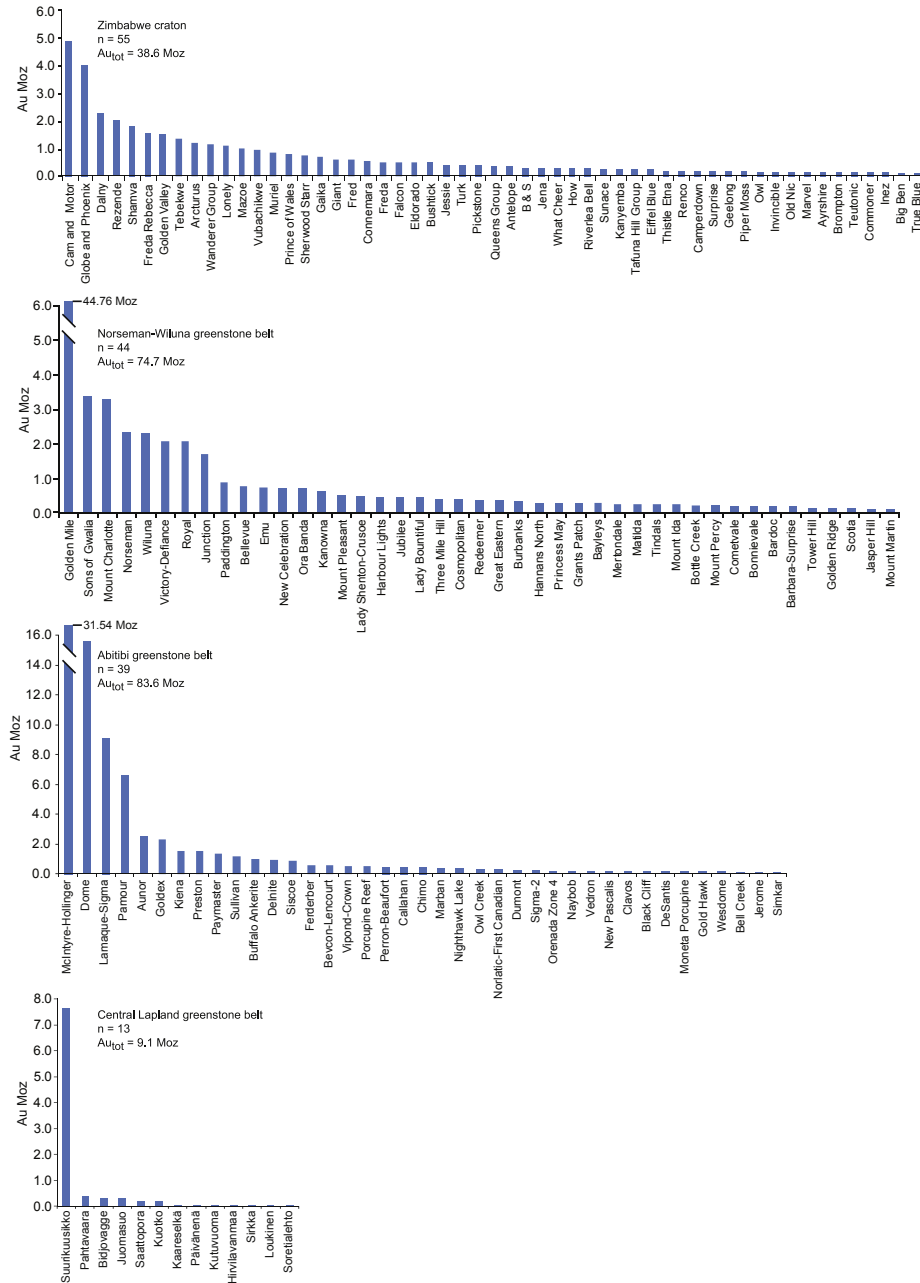


FIGURE 10.2.8 Resources of the known orogenic gold deposits in the Zimbabwe craton, Abitibi, Norseman-Wiluna, and Central Lapland greenstone belts.

Source: Data after Gosselin and Dube (2005) except for CLGB, which is from Table 10.2.1.

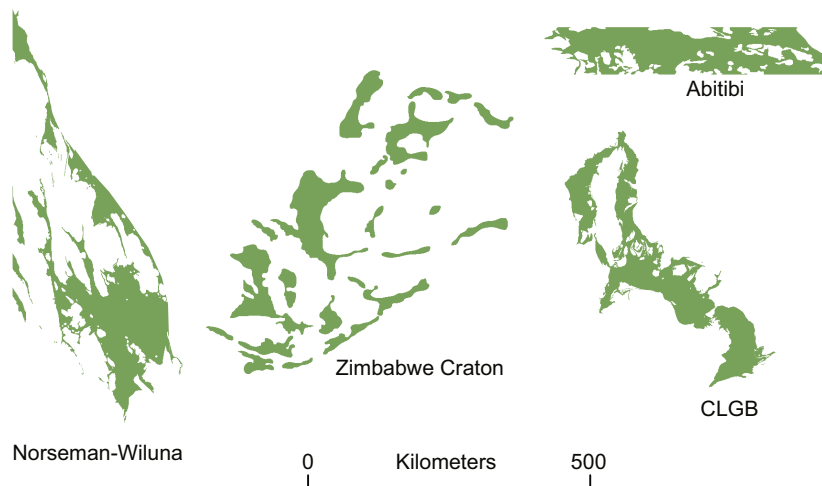


FIGURE 10.2.9 Size comparison of the Norseman-Wiluna, Abitibi, Central Lapland, and Zimbabwe Craton greenstone belts.

All belts presented are shown at the same scale.

Source: Modified and compiled after GTK Digital Bedrock Database, *Geological Survey of Western Australia (2010)*, *Robert et al. (2005)*, and *Pendergast (2003)*.

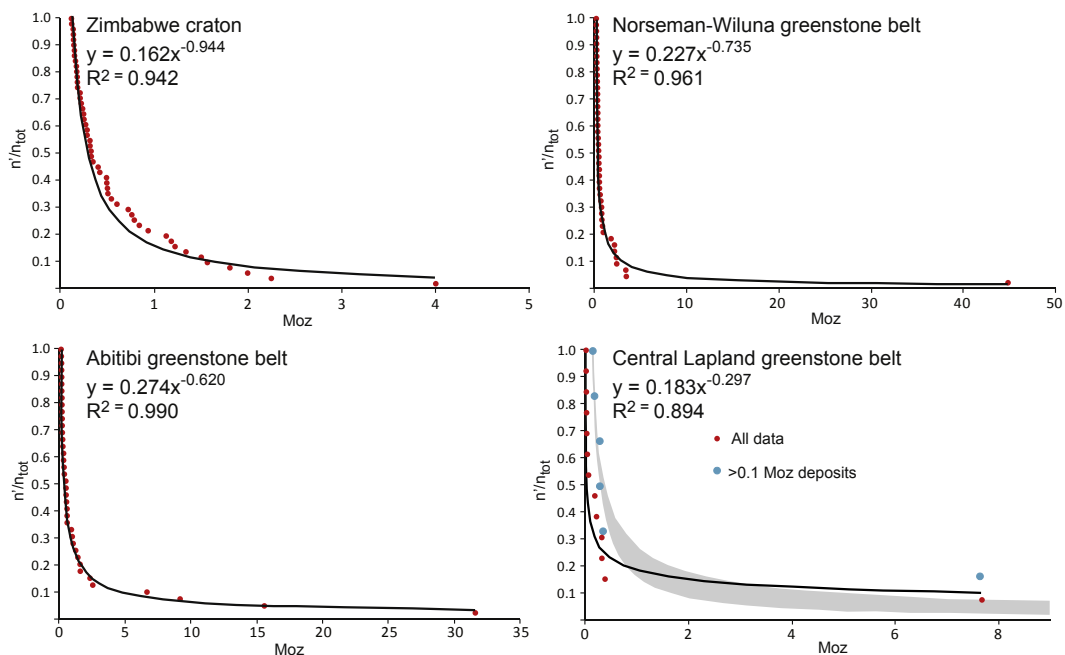


FIGURE 10.2.10 Regression plots of the gold districts and deposits shown in Fig. 10.2.8.

n = ordinal number of a deposit in the dataset from largest to smallest; n_{tot} = total number of deposits in the dataset; n/n_{tot} represents the probability of a deposit discovered being of same size or larger on the x -axis; Moz = size of the deposit in millions of troy ounces. Black lines are the regression line approximations fitted with least-squares method, formula, and correlation coefficient (R^2) shown in each case. The regression line fitted in the last panel is calculated using the whole dataset of the CLGB. The gray-shaded area in the CLGB panel shows the area covered by the fitted curves of other datasets. The CLGB data without subeconomic deposits is also plotted in the last panel, showing similarity with the data from other districts (see text).

contacts where they are exposed or drilled (e.g., [Hanski, 1997](#); [Lehtonen et al., 1998](#); [Hanski and Huhma, 2005](#)). If the Kittilä terrane represents a sequence of oceanic crust as suggested by [Hanski \(1997\)](#), the 9-km thickness in the central parts suggests a doubling of this part of the unit during deformation.

An increasing amount of evidence on the geological features of orogenic gold deposits indicates that they develop as a consequence of a regional metamorphic fluid flow event rather than being linked to local igneous activity (e.g., [Groves et al., 1998](#); [Goldfarb et al., 2005](#)). It has been clearly demonstrated that hydrothermal fluids identical to those that form orogenic gold deposits, as well as the gold and other metals enriched in orogenic gold deposits, are released via prograde metamorphism (e.g., [Pitcairn, 2006](#); [Philips and Powel, 2010](#)). The quantitative estimation presented in this work suggests that 20–30 times the currently known gold resources of the Kittilä terrane may have been mobilized during metamorphism from the Kittilä terrane rocks alone. Obviously, the mobilized gold needs to be focused into suitable structures and ultimately precipitated in appropriate traps. The efficiency of these processes is unknown, and some of the gold undoubtedly precipitated above the current erosion level.

In spite of the number of uncertainties and the hypothetical character of the calculations presented, it is believed that this modeling provides a good rough estimation of the gold potential of the Kittilä terrane. The calculations suggest that the orogenic gold deposits in the Kittilä terrane could have formed entirely via metamorphic processes and the sole source of gold can be the rocks that underwent metamorphism at depth. The data do not exclude the potential input of gold from intrusions or input from subducted crustal slab undergoing metamorphism at depth. All magmatic effects should have a positive effect on gold potential and gold mobility, either by adding heat, fluid, or gold to the system. Similarly, input from a potential subduction zone would have a positive effect on the gold budget. Calculations presented, however, suggest more than enough gold may have been mobilized from metamorphosed Kittilä terrane rocks alone to cover the currently known gold resources.

A statistical comparison of Abitibi, Norseman-Wiluna, and Zimbabwe greenstone belts indicate surprisingly coherent size distribution patterns between the belts. All of the districts are under active exploration and mining, and evidently there have been increases in the resources of actively explored deposits and new deposits since the database compilation of [Gosselin and Dubé \(2005\)](#). Although the new resources discovered in these areas will undoubtedly have minor effects on the distribution patterns, we find it very unlikely that the near-logarithmic fractal pattern detected will dramatically change. In our comparison, the differences in geological features (e.g., age, tectonic, and structural setting of the belts) was not taken in account. These features most certainly have an impact on total gold endowment of the respective district; however, based on the comparison presented, the size distribution of the deposits appears to be less affected. The comparison between the well-explored orogenic gold districts and CLGB presented in this work suggests that the size distribution of the gold deposits in the CLGB is significantly different from the other belts presented. Most likely this reflects the short exploration history and therefore a significant number of orogenic gold deposits still to be discovered in the belt. The number and size of those is unknown, but there is a clear gap between the current largest and second largest deposits of the CLGB.

SUMMARY

This study was aimed to establish the 3D shape of the Kittilä terrane, use the model generated to estimate its orogenic gold potential, and carry out a statistical comparison of the CLGB gold deposits with similar but more mature orogenic gold districts around the world.

Applying an in situ metamorphic source model for the orogenic gold deposits, the total amount of gold mobilized from the Kittilä terrane rocks during prograde metamorphism may have reached 143–228 Moz, roughly 20–30 times the amount of gold currently reported from the known deposits within the terrane. This indicates that at least in the Kittilä area, metamorphic processes alone could have potentially released enough gold to generate the known gold resources. However, magmatic input in the metal, fluid, or thermal budget of the system cannot be excluded, nor can the potential of subcrustal sources for metals and fluids be excluded. Should magmatic processes and/or additional deeper-sourced processes have been involved in the Kittilä area, they would have had a positive effect on the gold budget.

The statistics of the gold deposit sizes in the Norseman-Wiluna belt, Abitibi belt, and greenstone belts of the Zimbabwe craton indicate that the size distribution of gold deposits in certain districts appears to follow nonlinear distributions that bear similarities to the one outlined by the Gutenberg–Richter law for earthquakes. In comparison, the size distribution of the known gold deposits in CLGB is abnormal. Several gold deposits, including deposits in the size category of 0.5–1.5 Moz, need to be added to the CLGB dataset for it to follow the distribution pattern of the other datasets. This is assuming Suurikuusikko is the largest deposit. Should there be undiscovered deposits larger than Suurikuusikko, the gold potential will be considerably higher.

ACKNOWLEDGMENTS

The authors wish to thank Dr. David Groves for an insightful review, although he did not agree on all aspects of the modeling, and Dr. Hugh O'Brien for his editorial comments; both considerably improved the quality of the manuscript.

REFERENCES

- Agnico Eagle Ltd, 2013. Kittilä Mine resources and reserves as of December 31, 2012. <http://www.agnicoeagle.com/en/Operations/Northern-Operations/Kittila/Pages/default.aspx>.
- Bedrock of Finland – DigiKP. Digital map database [Electronic resource]. Geological Survey of Finland (referred 15th October 2013).
- Bonham-Carter, G.F., Agterberg, F.P., Wright, D.F., 1988. Integration of geological datasets for gold exploration in Nova Scotia. *Photogrammetric Engineering and Remote Sensing* 54 (77), 1585–1592.
- Eilu, P., Sorjonen-Ward, P., Nurmi, P., Niiranen, T., 2003. A review of gold mineralization styles in Finland. In: A group of papers devoted to the metallogeny of gold in the Fennoscandian Shield. *Economic Geology* 98, 1329–1353.
- Eilu, P., Pankka, H., Keinänen, V., et al., 2007. Characteristics of gold mineralisation in the greenstone belts of northern Finland. In: Ojala, J. (Ed.), *Gold in the Central Lapland Greenstone Belt*. Geological Survey of Finland. Special Paper 44, 57–106.
- Eilu, P., Ahtola, T., Äikäs, O., et al., 2012. Metallogenic areas in Finland. In: Eilu, P. (Ed.), *Mineral Deposits and Metallogeny of Fennoscandia*. Geological Survey of Finland, Special Paper 53, 207–342.
- FINGOLD – a public database on gold deposits in Finland [Electronic resource]. Geological Survey of Finland (referred 15th October 2013)
- Geological Survey of Western Australia, 2010. East Yilgarn, 2010 update: Geological Survey of Western Australia. Geological Information Series. 1:100,000.
- Goldfarb, R.J., Groves, D.I., Gardoll, S., 2001. Orogenic gold and geologic time: a global synthesis. *Ore Geology Reviews* 18, 1–75.

- Goldfarb, R.J., Baker, T., Dube, B., et al., 2005. Distribution, character, and genesis of gold deposits in metamorphic terranes. In: 100th Anniversary Volume of Economic Geology, pp. 407–450.
- Goldfarb, R.J., Santosh, M., 2014. The dilemma of the Jiaodong gold deposits: Are they unique? *Geoscience Frontiers* 5, 139–153.
- Gosselin, P., Dubé, B., 2005. Gold deposits of the world: distribution, geological parameters and gold content. Geological Survey of Canada. Open file 4895, 1 CD-ROM.
- Groves, D.I., Goldfarb, R.J., Gebre-Mariam, M., et al., 1998. Orogenic gold deposits: A proposed classification in the context of their crustal distribution and relationship to other gold deposit types. *Ore Geology Reviews* 13, 1–28.
- Groves, D.I., Goldfarb, R.J., Robert, F., Hart, G.J.R., 2003. Gold deposits in metamorphic belts: overview of current understanding, outstanding problems, future research, and exploration significance. *Economic Geology* 98, 1–30.
- Gutenberg, B., Richter, C.F., 1949. *Seismicity of the Earth and Associated Phenomena*. Princeton University Press, Princeton, NJ. 273.
- Hanski, E., 1997. The Nuttio serpentinite belt, Central Lapland: An example of Paleoproterozoic ophiolite mantle rocks in Finland. *Ophioliti* 22, 35–46.
- Hanski, E., Huhma, H., Vaasjoki, M., 2001. Geochronology of northern Finland: a summary and discussion. In: Vaasjoki, M. (Ed.), *Radiometric Age Determinations from Finnish Lapland and Their Bearing on the Timing of Precambrian Volcano-Sedimentary Sequences*. Geological Survey of Finland, Special Paper 33, 255–279.
- Hanski, E., Huhma, H., 2005. Central Lapland Greenstone Belt. In: Lehtinen, M., Nurmi, P.A., Rämö, O.T. (Eds.), *Precambrian Geology of Finland—Key to Evolution of the Fennoscandian Shield*. Elsevier, Amsterdam, pp. 139–194.
- Hölttä, P., Väisänen, M., Väänänen, J., Manninen, T., 2007. Paleoproterozoic metamorphism and deformation in central Lapland, Finland. In: Ojala, V.J. (Ed.), *Gold in the Central Lapland Greenstone Belt*. Geological Survey of Finland, Special Paper 44, 7–56.
- Korkiakoski, E., 1992. Geology and geochemistry of the metakomatiite-hosted Pahtavaara gold deposit in Sodankylä, northern Finland, with emphasis on hydrothermal alteration. Geological Survey of Finland, Bulletin 360, 96, 18 app.
- Kukkonen, I.T., Lahtinen, R. (Eds.), 2006. Finnish Reflection Experiment—FIRE 2001–2005. Special Paper 43. Geological Survey of Finland, Espoo, p. 247. plus 15 app. (CD-ROM).
- Kukkonen, I.T., Heikkinen, P., Heinonen, S., Laitinen, J., HIRE Working Group, 2011. In: Nenonen, K., Nurmi, P.A. (Eds.), *Geoscience for Society 125th Anniversary Volume*. Geological Survey of Finland, Special Paper 49, 49–58.
- Lahtinen, R., Korja, A., Nironen, M., 2005. Paleoproterozoic tectonic evolution. In: *Precambrian Geology of Finland—Key to the Evolution of the Fennoscandian Shield*. Developments in Precambrian Geology 14. Elsevier, Amsterdam, pp. 481–531.
- Lehtonen, M., Airo, M.-L., Eilu, P., et al. 1998. The stratigraphy, petrology and geochemistry of the Kittilä greenstone area, northern Finland. A report of the Lapland Volcanite Project. Geological Survey of Finland, Report of Investigation 140, p. 144 (in Finnish with summary in English).
- McCuaig, T.C., Kerrich, R., 1998. P-T-t-deformation-fluid characteristics of lode gold deposits: evidence from alteration systematics. *Ore Geology Reviews* 12, 381–453.
- Nykänen, V., Groves, D.I., Ojala, V.J., Gardoll, S.J., 2008. Combined conceptual/empirical prospectivity mapping for orogenic gold in the northern Fennoscandian Shield, Finland. *Australian Journal of Earth Sciences* 55 (1), 39–59.
- Patison, N.L., Korja, A., Lahtinen, R., Ojala, V.J., 2006. FIRE Seismic Reflection Profiles 4, 4A and 4B: Insights into the crustal structure of northern Finland from Ranua to Näätämö. In: Finnish Reflection Experiment (FIRE), 2001–2005. Geological Survey of Finland, Special Paper 43, 161–222.

- Patison, N.L., 2007. Structural controls on gold mineralisation in the Central Lapland Greenstone Belt. In: Ojala, V.J. (Ed.), *Gold in the Central Lapland Greenstone Belt*. Geological Survey of Finland, Special Paper 44, 107–124.
- Pendergast, M.D., 2003. The nickeliferous Late Archean reliance komatiitic event in the Zimbabwe craton—magmatic architecture, physical volcanology, and ore genesis. *Economic Geology* 98, 865–891.
- Philips, G.N., Powell, R., 2010. Formation of gold deposits: A metamorphic devolatilization model. *Journal of Metamorphic Geology* 28, 689–718.
- Pitcairn, I.K., Teagle, D.A.H., Craw, D., et al., 2006. Sources of metals and fluids in orogenic gold deposits: Insights from the Otago and Alpine schists, New Zealand. *Economic Geology* 101, 1525–1546.
- Pitcairn, I.K., 2012. Background concentrations of gold in different rock types. *Applied Earth Science* 120, 31–38.
- Rasilainen, K., Eilu, P., Karvinen, A., et al., 2012. Undiscovered orogenic gold resources in northern Finland. In: Hölttä, P. (Ed.), *Current Research: GTK Mineral Potential Workshop*, Kuopio, May. Geological Survey of Finland, Report of Investigation 198, pp. 141–145.
- Rastas, P., Huhma, H., Hanski, E., et al., 2001. U-Pb isotopic studies on the Kittilä greenstone area, central Lapland, Finland. In: Vaasjoki, M. (Ed.), *Radiometric age determinations from Finnish Lapland and their bearing on the timing of Precambrian volcano-sedimentary sequences*. Geological Survey of Finland, Special Paper 33, 95–141.
- Robert, F., Poulsen, H., Cassidy, K.F., Hodgson, C.J., 2005. Gold metallogeny of the Yilgarn and Superior cratons. *Economic Geology One Hundred Anniversary volume*. Society of Economic Geology 1001–1034.
- Singer, D.A., 1993. Basic concepts in three-part quantitative assessments of undiscovered mineral resources. *Non-renewable Resources* 2, 69–81.
- Singer, D.A., Menzie, W.D., 2010. *Quantitative Mineral Resource Assessments: An Integrated Approach*. Oxford University Press, New York. 219.
- Tuisku, P., Mikkola, P., Huhma, H., 2006. Evolution of migmatitic granulite complexes: implications from Lapland granulite belt, Part 1: Metamorphic geology. *Bulletin of the Geological Society of Finland* 78, 71–105.
- Väisänen, M., 2002. Structural features in the central Lapland greenstone belt, northern Finland. Geological Survey of Finland, Report K 21.42/2002/3; p. 20, 16 app.
- Vanhanen, E., 2001. Geology, mineralogy and geochemistry of the Fe-Co-Au-(U) deposits in the Paleoproterozoic Kuusamo schist belt, northeastern Finland. Geological Survey of Finland, Bulletin 399, p. 229, 13 app., 1 app., and map.
- Ward, P., Härkönen, I., Nurmi, P.A., Pankka, H.S., 1989. Structural studies in the Lapland greenstone belt, northern Finland and their application to gold mineralization. In: Geological Survey of Finland. *Current Research*, 1988. Geological Survey of Finland, Special Paper 10, 71–77.